Chiral-Selective Formation of 1D Polymers Based on Ullmann-Type Coupling: The Role of the Metallic Substrate

Tuan Anh Pham, Bay V. Tran, Manh-Thuong Nguyen, and Meike Stöhr**

The chiral-selective formation of 1D polymers from a prochiral molecule, namely, 6,12-dibromochrysene in dependence of the type of metal surface is demonstrated by a combined scanning tunneling microscopy and density functional theory study. Deposition of the chosen molecule on Au(111) held at room temperature leads to the formation of a 2D porous molecular network. Upon annealing at 200 °C, an achiral covalently linked polymer is formed on Au(111). On the other hand, a chiral Cu-coordinated polymer is spontaneously formed upon deposition of the molecules on Cu(111) held at room temperature. Importantly, it is found that the chiral-selectivity determines the possibility of obtaining graphene nanoribbons (GNRs). On Au(111), upon annealing at 350 °C or higher cyclo-dehydrogenation occurs transforming the achiral polymer into a GNR. In contrast, the chiral coordination polymer on Cu(111) cannot be converted into a GNR.

1. Introduction

Chirality is a fundamental topic which is important in many areas of science and engineering, including chemistry, biology, pharmacology, and surface science.[1] Thus, detailed insight into chiral phenomena is of utmost importance for the effective usage of chiral systems in potential future applications, such as nonlinear optics, enantioselective heterogeneous catalysis, enantiospecific sensors, or liquid-crystal display technologies.[2] In this context, probing low-dimensional chiral architectures consisting of chiral or prochiral molecular precursors adsorbed at solid surfaces using scanning tunneling microscopy (STM) is nowadays considered as one of the most powerful and appropriate approaches to obtain an in-depth understanding of different chirality aspects at the single molecule scale.[3] To date, various chiral phenomena (e.g., chiral switching, spontaneous chiral resolution, or chiral amplification) of different chiral supramolecular architectures on solid surfaces, including clusters, 1D structures, or 2D arrays have been intensively investigated.[4] Despite these significant achievements, however, controlling and understanding chirality in on-surface chemical reactions has been hardly studied and thus, more investigations are urgently needed. It has been recognized that the formation of new bonding motifs in on-surface chemical reactions—also in dependence of the chemical nature of the chosen substrate—may significantly impact chirality phenomena at solid surfaces.[5]

Herein, we report, through a combination of STM measurements and density functional theory (DFT) calculations the chiral-selective formation of 1D polymers depending on the choice of metal surface using Ullmann-type coupling under ultrahigh vacuum (UHV) conditions. For this purpose, 6,12-dibromochrysene (DBCh) was selected as the starting molecular building block, while Au(111) and Cu(111) were employed as substrates because of their significant differences in chemical reactivity.[6] Notably, DBCh is prochiral in the gas or liquid phase but it becomes chiral upon adsorption

Dr. T. A. Pham, Dr. B. V. Tran, Prof. M. Stöhr
Zernike Institute for Advanced Materials
University of Groningen
Nijenborgh 4, 9747 AG, Groningen, The Netherlands
E-mail: t.a.pham@rug.nl; m.a.stohr@rug.nl
Dr. M.-T. Nguyen
Center for Computational Physics
Institute of Physics
Vietnam Academy of Science and Technology
10 Dao Tan St., Hanoi, Vietnam

DOI: 10.1002/smll.201603675

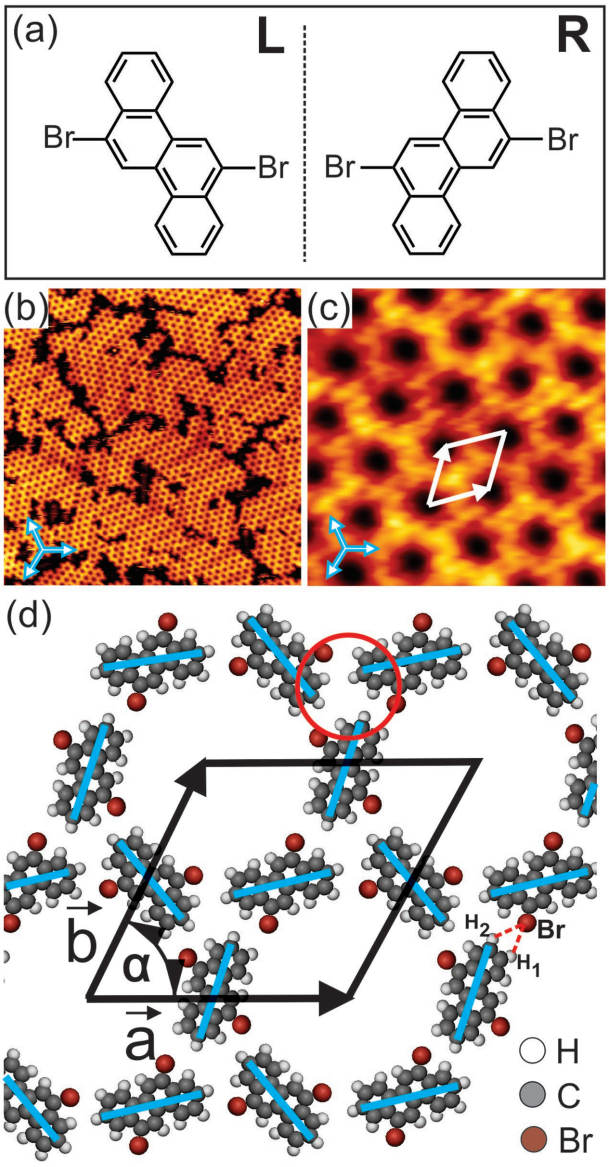

Figure 1. a) Chemical structure of DBCh showing the two possible enantiomers (labeled L and R) when adsorbed on a surface. b,c) Overview and close-up STM images (100×100 nm^2 and 12×12 nm^2, respectively) of the 2D porous network for close to 1 ML coverage on Au(111). d) Tentative model for the porous network. The unit cell vectors are denoted by white and black arrows in (c) and (d), respectively. The blue bars in (d) represent the orientation of the molecules in the network. The set of three arrows indicates the principal directions of the underlying substrate.

at solid surfaces due to dimensionality reduction. Therefore, the left- and right-handed enantiomer of DBCh can be distinguished on the surface since it either adsorbs face-up or face-down (labeled as L and R, respectively, in **Figure 1**a).[7]

2. Results and Discussion

Upon deposition of DBCh on Au(111) held at room temperature (RT), a 2D porous self-assembled molecular network was observed by STM under UHV conditions (Figure 1b). The porous network is similar for both sub-monolayer and close to a full monolayer (1 ML) coverage (Figure S1, Supporting Information). Notably, the characteristic herringbone reconstruction of Au(111) is visible through the molecular adlayer. The Au reconstruction is neither modified nor lifted upon adsorption of the molecules, indicating a weak molecule–substrate interaction.[8] In the close-up STM image (Figure 1c), individual pores in the 2D porous molecular network are visible. As determined from the STM measurements, the molecules are arranged in a rhombic unit cell with dimensions of $a = b = (25 \pm 1.4)$ Å and an internal angle $\alpha = (60 \pm 3)°$. It should be noted that one axis of the molecular unit cell is rotated by $(14 \pm 2)°$ with respect to a principal Au direction. Thus, it can be expected that for each domain of the porous network a mirror domain exists and a principal Au direction acts as the mirror axis. That implies that each domain is chiral and consists of either the L or the R enantiomer. Indeed, we observed the existence of mirror domains A_m, which are mirrored at a principal Au direction and which are the counterpart of domains A (see Figure S2, Supporting Information). The unit cell directions of "normal" and mirror domains enclose an angle of $\pm(14\pm2)°$ with a principal Au direction. Figure 1d depicts the tentative molecular model for the observed 2D porous molecular network on Au(111) (see also Figure S3, Supporting Information). In this model, each pore consists of six molecules rotated by 120° with respect to each other. Three neighboring molecules point toward each other to form a threefold node (marked by a red circle in Figure 1d). Each molecule connects to two such threefold nodes. The 2D porous molecular network is stabilized by a triangular binding motif based on hydrogen bonding enabled by the opposite charge regions of Br and H atoms within the threefold nodes (e.g., Br$-$H$_2-$H$_1$ in Figure 1d).[9] These findings are strongly supported by our gas-phase DFT calculations where the dimensions of the calculated unit cell as well as the Br to H distances are in accordance with the experimental results (see Figure S4, Supporting Information, for detailed information).

Annealing sub-monolayer coverage of DBCh adsorbed on Au(111) at 200 °C results in the formation of 1D polymers, which exhibit variable lengths (**Figure 2**a). Interestingly, most of the newly formed 1D polymers are isolated on the surface and align parallel to the herringbone reconstruction (Figure 2a and Figure S5a, Supporting Information). It has been previously reported that depending on the molecular precursor employed for Ullmann-type coupling, such 1D polymers obtained after annealing at around 200 °C (i.e., the debromination reaction proceeded) can be stabilized by either Au–ligand coordination bonds or C$-$C covalent bonds.[10] The close-up STM image in Figure 2b clearly reveals that the 1D polymer exhibits a zigzag shape which is due to the alternating arrangement of left- and right-handed enantiomers. Two opposite handed enantiomers connect to each other to form a dimer, which can be considered as the basic unit for the formation of the 1D polymer. To shed light onto the polymer formation, we performed DFT calculations for the dimeric units taking the Au(111) substrate into account (Figure 2d). It turns out that the heterochiral covalently coupled dimer (LR1C) is found to be 0.65 and 0.05 eV more stable than the

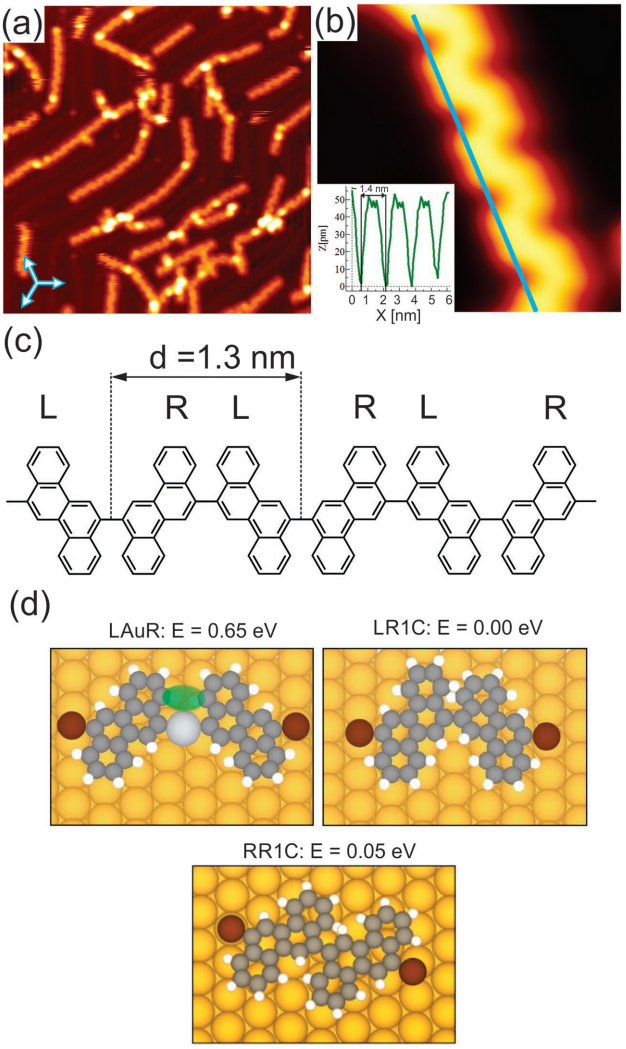

Figure 2. a) Overview STM image (50×50 nm^2) showing the formation of 1D polymers of DBCh on Au(111) after annealing at 200 °C. The set of three arrows indicates the principal directions of the underlying substrate. b) Close-up STM image (6×6 nm^2) of a 1D polymer strand. The inset in (b) displays the line profile along the blue line. c) Proposed molecular model for the 1D polymer of DBCh on Au(111). The repeat distance of d = 1.3 nm is the value obtained from DFT. d) DFT results for the optimized geometry for a metal-coordinated (LAuR) and the covalently linked dimers LR1C and RR1C on Au(111). The metal adatom is represented by a gray sphere. The distance between the two closest H atoms in the LAuR dimer is marked by a green oval.

Au-coordinated one (LAuR) and the homochiral covalently coupled one (RR1C), respectively. Note that the 0.05 eV difference in energy between the LR1C and RR1C structures is negligible. However, the experimentally determined basic unit length is found to be (1.4 ± 0.1) nm (inset in Figure 2b), which agrees well with the results obtained by our DFT calculations (1.3 nm) for the optimized geometry of the covalently coupled dimer in the case of LR1C. This value is much larger than the one of 0.66 nm in the case of RR1C. Notably, it has been previously reported that the formation of Au-coordinated polymers on Au(111) can lead to the rearrangement of the herringbone reconstruction.[11] However, in our case the herringbone reconstruction is unaffected upon the 1D polymer formation. These findings, therefore, unambiguously suggest that upon thermal annealing the C–Br bonds are dissociated and a 1D covalently linked polymer forms on Au(111) based on Ullmann-type coupling. The molecular model for the newly formed 1D polymer is shown in Figure 2c. In this model, the 1D polymer stabilized by covalent C–C bonding is achiral with an alternating arrangement of left- and right-handed enantiomers. Thus, the chirality of the monomers is transferred by the on-surface reaction into the polymer. It is assumed that the LR1C coupling is energetically more favorable than the RR1C coupling. This may be the main reason for the transformation of the 2D homochiral self-assembled network into the 1D heterochiral polymer on Au(111) after annealing at 200 °C.

Additional annealing of the sample at higher temperatures results in significant changes in the morphology of the newly formed polymer. In the studied temperature range between 350 and 400 °C, a considerable number of branched and interconnected polymers was observed by STM (marked by blue circles in Figure S5, Supporting Information). That is in contrast to the isolated 1D polymers found on Au(111) for annealing at around 200 °C. It has been recently reported that the formation of such complex polymer architectures is due to the chemical cross-linking between the already formed polymer segments on Au(111) induced by cyclo-dehydrogenation reactions (see the molecular model in Figure S6, Supporting Information).[12] More interestingly, by applying a derivative filter (first derivative along the axis of the 1D polymer) for STM images taken for samples, which were annealed at 200 and 350 °C, respectively, we were able to determine for which annealing temperature GNR formation happened. For annealing temperatures in the range of 200 °C, opposite tilting of neighboring binaphthyl groups was detected: within each dimer unit a darker and a brighter protrusion is visible (**Figure 3**a). This is an indication that due to steric repulsion between the hydrogen atoms of adjacent 2,2′-binaphthyl units a rotation of the binaphthyl units around the σ-bonds connecting them happens and thus, no cyclo-dehydrogenation occurred yet. However, such a difference in the apparent height of the binaphthyl units was not observed for annealing at 350 °C (see Figure 3b and profile analysis in Figure S7, Supporting Information). From this observation we conclude that a fully aromatic system formed via cyclo-dehydrogenation. This result is in excellent agreement with a previous report on the formation of GNRs from bianthryl precursors on Au(111).[10b] We would like to point out that kinks and crossings of the graphene nanoribbons normally consist of carbon pentagons and heptagons as demonstrated by previous reports.[12b] Thus, on the basis of this observation, it is suggested that the 1D covalently linked polymers formed on Au(111) at 200 °C were converted into so-called graphene nanoribbons through cyclo-dehydrogenation reactions at annealing temperatures of 350 °C or higher. The molecular models for both covalently linked polymer networks and graphene nanoribbons are shown in Figure 3 and Figure S6 (Supporting Information).

To examine the influence of the metal substrate on the structural formation of the polymers of DBCh, Cu(111) was employed as a substrate because its reactivity is generally

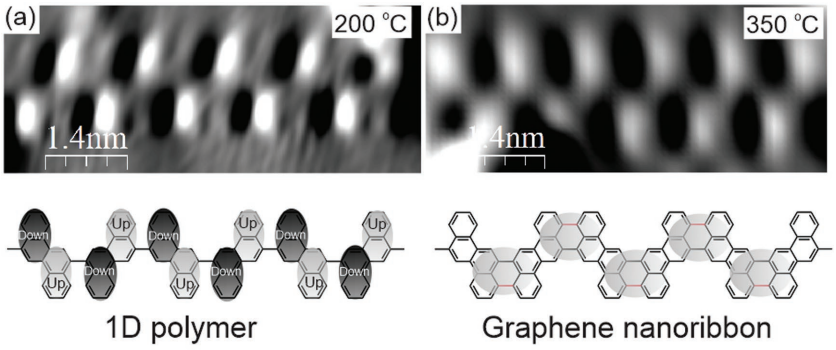

Figure 3. Close-up STM images obtained by applying a derivative filter along the *x*-axis and the corresponding molecular models for the a) covalently linked 1D polymer formed at 200 °C after the debromination reaction and b) graphene nanoribbons formed at 350 °C after the cyclo-dehydrogenation. The opposite tilting of neighboring binaphthyl units in the covalently linked 1D polymer can be discerned and is marked by gray (tilt-up) and black ovals (tilt-down) in the molecular model (a). In contrast, no tilting of the binaphthyl units was observed in the case of graphene nanoribbons as can be seen from the molecular model in (b) (gray ovals).

considered to be higher than the one of Au(111).[6] Upon deposition of DBCh on Cu(111) held at RT, 1D polymers were observed (**Figure 4**a), regardless of the molecular coverage (Figure S8, Supporting Information). Interestingly, the presence of vacancies in the Cu surface was clearly observed (Figure S9, Supporting Information). The depth of the vacancies amounts to about 1.8 Å, which is equal to the height of a monoatomic step of the Cu(111) surface (1.9 Å). The presence of such vacancies can be regarded as a preliminary sign of the incorporation of Cu atoms into the newly formed polymer.[13a] In the close-up STM image in Figure 4b, individual monomers within the 1D polymer can be clearly discerned. It is apparent that the 1D polymer chains consist of only one type of enantiomer connected to each other in a linear fashion. Notably, previous studies for on-surface polymerization of brominated precursors on Cu(111) demonstrated that the Br atoms can be split-off from the C–Br bonds upon adsorption on Cu(111) held at RT, promoting the formation of Cu-coordinated polymer networks based on Ullmann-type coupling.[13] To gain detailed insight into the structural formation of the 1D polymers on Cu(111), the monomer-to-monomer distance was measured and then compared to the results obtained by DFT calculations for the dimer unit in the case of a Cu-coordinated structure (RCuR in Figure 4d). The experimentally measured distance between two monomers is found to be (1.0 ± 0.1) nm (inset in Figure 4b), which is in good agreement with the computationally determined monomer-to-monomer distance for the optimized geometry of the Cu-coordinated dimer (0.9 nm). Thus, it can be concluded that a 1D organometallic polymer spontaneously forms on Cu(111) enabled through the debromination of DBCh at RT which is facilitated by the comparably high catalytic activity of the Cu surface. The suggested molecular model for the 1D organometallic polymer formed on Cu(111) is shown in Figure 4c. The 1D organometallic polymer consists of only one type of enantiomer (either L- or R-DBCh) and thus, each polymer strand is chiral. In STM we observed the coexistence of both left- and right-handed polymers on Cu(111) at the same time (Figure S10, Supporting Information). Comparing the results obtained for Ullmann-type coupling of DBCh on Au(111) and Cu(111) we conclude that a chiral-selective formation occurs for the 1D polymers in dependence of the substrate. A potential reason may be the formation of different bonding motifs upon the on-surface coupling reaction on Au(111) and Cu(111) (C–C covalent bonds and C–Cu–C coordination bonds, respectively). For the case of the chiral 1D organometallic polymers on Cu(111), most polymers align within an angle of ±10° along the ⟨11-2⟩ directions of the Cu(111) substrate (Figure 4a and Figure S11, Supporting Information). For the chiral 1D polymer the Cu adatoms arrange linearly and if a commensurate arrangement of the monomers is assumed the adatoms are then always adsorbed on the same lattice sites. In contrast, if achiral 1D organometallic polymers would form, the Cu adatoms would describe a zigzag line and a commensurate arrangement of the adatoms would be no longer possible (see Figure S12, Supporting Information). Different adsorption sites of the adatoms for the achiral polymer could be slightly less preferred and thus, the chiral organometallic polymers would be favored.

In order to obtain additional information on the chiral-selective 1D polymer formation on Cu(111), we carried out DFT calculations for the dimeric units for both cases, the chiral and achiral Cu-coordinated structures (labeled RCuR and LCuR, respectively, in Figure 4d). It turned out that the achiral Cu-coordinated structure is found to be 0.18 eV less stable than the chiral Cu-coordinated one. In view of steric repulsion between the hydrogen atoms of neighboring monomers this is very reasonable. The distance between the two closest H atoms is in the case of the achiral structure (1.9 Å) much smaller compared to the case of the chiral structure (3.1 Å). Furthermore, the angle of the chiral polymer with the ⟨11-2⟩ Cu directions amounts to 7° which fits very well with the experimentally determined parameter.

Annealing the sample on Cu(111) at 250 °C in order to probe if the Cu-coordinated 1D polymers can be transformed into covalently coupled ones led to the presence of disordered networks and clusters on the surface. Deposition of the molecules on a Cu(111) surface kept at elevated temperatures (T > 200 °C) led to a similar result (Figure S13, Supporting Information). It has been previously reported that annealing Cu-coordinated polymer networks formed on Cu(111) at temperatures between 200 and 250 °C results in the formation of graphene nanoribbons induced by cyclodehydrogenation.[14] However, such graphene nanoribbons were not observed on Cu(111) in our case. This result is in contrast to the formation of graphene nanoribbons on Au(111) for annealing at a temperature of 350 °C. This difference might be related to the formation of a chiral 1D polymer on Cu(111) upon debromination compared to an

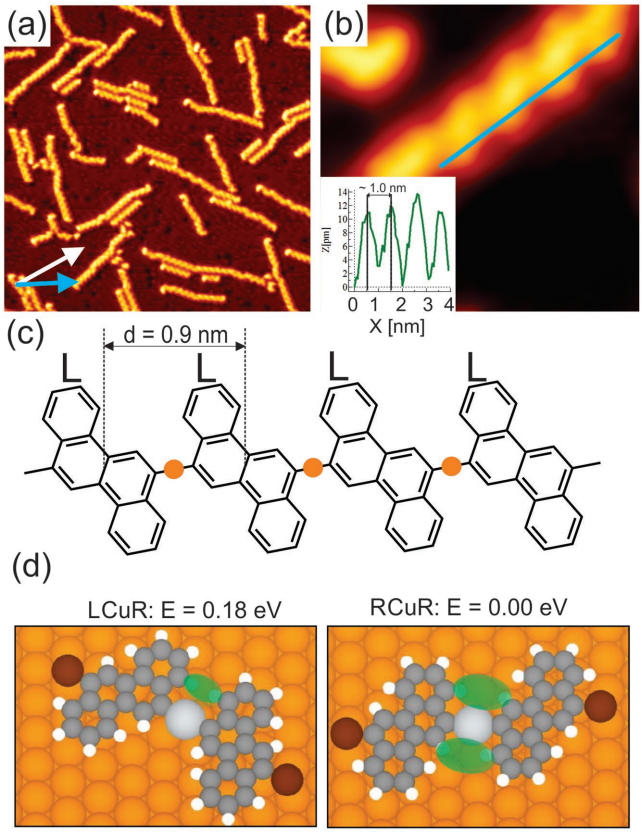

Figure 4. a) Overview STM image (50×50 nm^2) showing the formation of 1D polymers of DBCh on Cu(111) at RT. b) Close-up STM image (6×6 nm^2) for a 1D polymer. The inset in (b) shows the line profile along the blue line. (c) Proposed molecular model for the 1D polymer of DBCh on Cu(111). The repeat distance of $d = 0.9$ nm is the value obtained from DFT calculations. Filled orange circles represent Cu adatoms in the 1D organometallic polymer. The ⟨1-10⟩ and ⟨11-2⟩ substrate directions are denoted by blue and white arrows in (a), respectively. d) DFT results for the optimized geometry for an achiral (LCuR) and a chiral Cu-coordinated (RCuR) DBCh dimer on Cu(111). The metal adatoms are represented by gray spheres. The distances between the two closest H atoms in these dimers are marked by green ovals.

achiral one on Au(111). To gain additional insight, DFT calculations were performed to determine if a chiral or an achiral polymer structure would be energetically preferred. It turned out that the potential transformation of the chiral organometallic polymer into a covalently linked one is based on a five-membered C ring (RR2C in **Figure 5**). On the other hand, for the achiral organometallic polymer a six-membered C ring links the monomeric units (LR2C in Figure 5). From an energetic point of view the achiral polymer is 0.87 eV more stable than the chiral one and thus, is favored (Figure 5). Since in our case the starting point is a chiral polymer, the calculations can explain why no graphene nanoribbons are observed on Cu(111) after annealing at elevated temperatures.

3. Conclusion

In conclusion, we report for the first time a chiral-selective formation of 1D polymers based on Ullmann-type coupling for the case of DBCh on Au(111) versus Cu(111). Our study suggests that the bond formation (covalent vs coordination bonding) upon on-surface coupling reactions could be the main reason for the observed chiral selectivity. This is reflected by the formation of achiral 1D polymers based on covalent C–C bonds on Au(111), while the chiral 1D polymers on Cu(111) are stabilized by C–Cu–C coordination bonds. Interestingly, we found that the chiral-selectivity also influences the possibility to generate graphene nanoribbons which is possible on Au(111) but not on Cu(111). Thus, our findings represent an interesting example for chiral selectivity in on-surface synthesis and may inspire further work at the interface of chirality and on-surface synthesis.

4. Experimental Section

The STM experiments were carried out in a two-chamber ultra-high vacuum system with a base pressure of 5×10^{-11} mbar. The system houses a low-temperature STM (Scienta Omicron) equipped with facilities for surface preparation; that is, Ar^+ ion sputtering and resistive sample heating. The Au(111) and Cu(111) single crystals were prepared by repeated cycles of sputtering with Ar^+ ions and annealing at ≈450 and 500 °C, respectively. Commercially available 6,12-dibromochrysene (Sigma-Aldrich) was thoroughly degassed several hours before deposition onto the chosen substrate. The molecules were thermally evaporated from a glass crucible that was heated inside a home-built evaporator. The deposition rate was monitored using a quartz crystal microbalance in order to determine the molecular coverage. The substrate was held at room temperature during deposition. The STM images were taken in constant current mode at 77 K (typical scanning parameters were $U = -1.8$ V, $I = 20$ pA) using a platinum–iridium tip. Image processing was done with the free software WS×M.[15] 1 ML on Au(111) is defined as the whole Au(111) surface covered by the self-assembled porous molecular network. On Cu(111), however, 1 ML is defined as the whole Cu(111) surface covered by 1D polymers spontaneously formed upon deposition.

DFT calculations were carried out using the PBE density functional[16] corrected with van der Waals potentials.[17] The mixed Gaussian and plane-wave (GPW) hybrid basis set[18] was used: the localized Gaussian-based DZVP and plane-waves of 400 Ry cut off. Calculations were performed using the CP2K package.[19] Here, Au/Cu slabs of $5 \times 7/5 \times 8$ periodicity and of four metal layers (280/320 Au/Cu atoms) were used, in which the

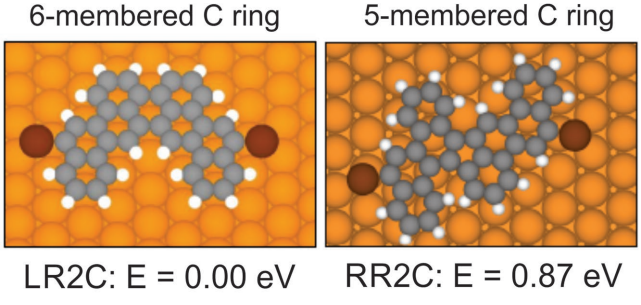

Figure 5. DFT calculated results for DBCh on Cu(111) showing that RR coupling results in a five-membered C ring, which is less stable than a six-membered C ring obtained in LR coupling.

two bottom layers were fixed in their bulk position in geometry optimizations.

Supporting Information

Supporting Information is available from the Wiley Online Library or from the author.

Acknowledgements

T.A.P., B.V.T., and M.S. acknowledge financial support from the Netherlands Organization for Scientific Research (NWO, Chemical Sciences, VIDI Grant No. 700.10.424) and the European Research Council (ERC-2012-StG 307760-SURFPRO).

[1] a) M. Liu, L. Zhang, T. Wang, *Chem. Rev.* **2015**, *115*, 7304; b) L. A. Nguyen, H. He, C. P. Huy, *Int. J. Biomed. Sci.* **2006**, *2*, 85; c) R. Corradini, S. Sforza, T. Tedeschi, R. Marchelli, *Chirality* **2007**, *19*, 269; d) K. H. Ernst, *Phys. Status Solidi B* **2012**, *249*, 2957; e) W. Xu, R. E. K. Kelly, H. Gersen, E. Lægsgaards, L. Stensgaard, L. N. Kantorovich, F. Besenbacher, *Small* **2009**, *5*, 1952; f) J. A. A. W. Elemens, I. D. Cat, H. Xu, S. De Feyter, *Chem. Soc. Rev.* **2009**, *38*, 722; g) L. Zhang, T. Wang, Z. Shen, M. Liu, *Adv. Mater.* **2016**, *28*, 1044; h) F. Zaera, *J. Phys. Chem. C* **2008**, *112*, 16196.

[2] a) L. M. Haupert, G. J. Simpson, *Annu. Rev. Phys. Chem.* **2009**, *60*, 345; b) T. P. Yoon, E. N. Jacobsen, *Science* **2003**, *299*, 1691; c) J. A. Switzer, H. M. Kothari, P. Poizot, S. Nakanishi, E. W. Bohannan, *Nature* **2003**, *425*, 490; d) R. P. Lemieux, *Acc. Chem. Res.* **2001**, *34*, 845; e) S. Pieraccini, S. Masiero, A. Ferrarini, G. P. Spada, *Chem. Soc. Rev.* **2011**, *40*, 258.

[3] a) R. Fasel, M. Parschau, K. H. Ernst, *Nature* **2006**, *439*, 449; b) S. De Feyter, P. C. M. Grim, M. Rücker, P. Vanoppen, C. Meiners, M. Sieffert, S. Valiyaveettil, K. Müllen, F. C. De Schryver, *Angew. Chem., Int. Ed.* **1998**, *37*, 1223; c) M. O. Lorenzo, C. J. Baddeley, C. Muryn, R. Raval, *Nature* **2000**, *404*, 376; d) A. G. Mark, M. Forster, R. Raval, *Tetrahedron: Asymmetry* **2010**, *21*, 1125; e) S. Weigelt, C. Busse, L. Petersen, E. Rauls, B. Hammer, K. V. Gothelf, F. Besenbacher, T. R. Linderoth, *Nat. Mater.* **2006**, *5*, 112; f) Q. Chen, N. V. Richardson, *Nat. Mater.* **2003**, *2*, 324; g) S. M. Barlow, R. Raval, *Surf. Sci. Rep.* **2003**, *50*, 201.

[4] a) P. Messina, A. Dmitriev, N. Lin, H. Spillmann, M. Abel, J. V. Barth, K. Kern, *J. Am. Chem. Soc.* **2002**, *124*, 14000; b) F. Vidal, E. Delvigne, S. Stepanow, N. Lin, J. V. Barth, K. Kern, *J. Am. Chem. Soc.* **2005**, *127*, 10101; c) M. Stöhr, S. Boz, M. Schär, M.-T. Nguyen, C. A. Pignedoli, D. Passerone, W. B. Schweizer, C. Thilgen, T. A. Jung, F. Diederich, *Angew. Chem., Int. Ed.* **2011**, *50*, 9982; d) A. Shchyrba, M.-T. Nguyen, C. Wäckerlin, S. Martens, S. Nowakowska, T. Ivas, J. Roose, T. Nijs, S. Boz, M. Schär, M. Stöhr, C. A. Pignedoli, C. Thilgen, F. Diederich, D. Passerone, T. A. Jung, *J. Am. Chem. Soc.* **2013**, *135*, 15270; e) K. Sun, T. N. Shao, J. L. Xie, M. Lan, H. K. Yuan, J. H. Xiong, J. Z. Wang, Y. Liu, Q. K. Xue, *Small* **2012**, *8*, 2078.

[5] a) G. P. Lopinski, D. J. Moffat, D. D. M. Wayner, R. A. Wolkow, *Nature* **1998**, *392*, 909; b) Y. J. Hwang, A. Kim, E. Hwang, S. Kim, *J. Am. Chem. Soc.* **2005**, *127*, 5016; c) P. Han, K. Akagi, F. F. Canova, H. Mutoh, S. Shiraki, K. Iwaya, P. S. Weiss, N. Asao, T. Hitosugi, *ACS Nano* **2014**, *8*, 9181; d) P. Han, K. Akagi, F. F. Canova, H. Mutoh, S. Shiraki, K. Iwaya, P. S. Weiss, N. Asao, T. Hitosugi, *ACS Nano* **2015**, *9*, 12035; e) H. Sakaguchi, S. Song, T. Kojima, T. Nakae, *Nat. Chem.* **2017**, *9*, 57.

[6] F. S. Tautz, *Prog. Surf. Sci.* **2007**, *82*, 479.

[7] a) H. Bertrand, F. Silly, M. P. Teulade-Fichou, L. Tortech, D. Fichou, *Chem. Commun.* **2011**, *47*, 10091; b) F. Grillo, J. A. G. Torres, M.-J. Treanor, C. R. Larrea, J. P. Götze, P. Lacovig, H. A. Früchtl, R. Schaub, N. V. Richardson, *Nanoscale* **2016**, *8*, 9167; c) J. Prinz, O. Gröning, H. Brune, R. Widmer, *Angew. Chem., Int. Ed.* **2015**, *54*, 3902; d) Y. Wei, K. Kannappan, G. W. Flynn, M. B. Zimmt, *J. Am. Chem. Soc.* **2004**, *126*, 5318.

[8] T. A. Pham, F. Song, M. Stöhr, *Phys. Chem. Chem. Phys.* **2014**, *16*, 8881.

[9] T. A. Pham, F. Song, M.-T. Nguyen, M. Stöhr, *Chem. Commun.* **2014**, *50*, 14089.

[10] a) H. Zhang, H. Lin, K. Sun, L. Chen, Y. Zagranyarski, N. Aghdassi, S. Duhm, Q. Li, D. Zhong, Y. Li, K. Müllen, H. Fuchs, L. Chi, *J. Am. Chem. Soc.* **2015**, *137*, 4022; b) J. Cai, P. Ruffieux, R. Jaafar, M. Bieri, T. Braun, S. Blankenburg, M. Muoth, A. P. Seitsonen, M. Saleh, X. Feng, K. Müllen, R. Fasel, *Nature* **2010**, *466*, 470; c) L. Grill, M. Dyer, L. Lafferentz, M. Persson, M. V. Peters, S. Hecht, *Nat. Nanotechnol.* **2007**, *2*, 687; d) A. Batra, D. Cvetko, G. Kladnik, O. Adak, C. Cardoso, A. Ferretti, D. Prezzi, E. Molinari, A. Morgante, L. Venkataraman, *Chem. Sci.* **2014**, *5*, 4419.

[11] a) A. Saywell, W. Gren, G. Franc, A. Gourdon, X. Bouju, L. Grill, *J. Phys. Chem. C* **2014**, *118*, 1719; b) H. Zhang, J.-H. Franke, D. Zhong, Y. Li, A. Timmer, O. D. Arado, H. Mönig, H. Wang, L. Chi, Z. Wang, K. Müllen, H. Fuchs, *Small* **2014**, *10*, 1361.

[12] a) P. Ruffieux, S. Wang, B. Yang, C. S. Sánchez, J. Liu, T. Dienel, L. Talirz, P. Shinde, C. A. Pignedoli, D. Passerone, T. Dumslaff, X. Feng, K. Müllen, R. Fasel, *Nature* **2016**, *531*, 489; b) A. Kimouche, M. M. Ervasti, R. Drost, S. Halonen, A. Harju, P. M. Joensuu, J. Sainio, R. Liljeroth, *Nat. Commun.* **2015**, *6*, 10177; c) T. Dienel, S. Kawai, H. Söde, X. Feng, K. Müllen, P. Ruffieux, R. Fasel, O. Gröning, *Nano Lett.* **2015**, *15*, 5185.

[13] a) T. A. Pham, F. Song, M.-T. Nguyen, Z. Li, F. Studener, M. Stöhr, *Chem. Eur. J.* **2016**, *22*, 5937; b) Q. Fan, C. Wang, Y. Han, J. Zhu, J. Kuttner, G. Hilt, J. M. Gottfried, *ACS Nano* **2014**, *8*, 709; c) W. Wang, X. Shi, S. Wang, M. Van Hove, N. Lin, *J. Am. Chem. Soc.* **2011**, *133*, 13264; d) M. Chen, J. Xiao, H. P. Steinrück, S. Wang, W. Wang, N. Lin, W. Hieringer, J. M. Gottfried, *J. Phys. Chem. C* **2014**, *118*, 6820.

[14] a) K. A. Simonov, N. A. Vinogradov, A. S. Vinogradov, A. Generalov, E. M. Zagrebina, G. I. Svirskiy, A. A. Cafolla, T. Carpy, J. P. Cunniffe, T. Taketsugu, A. Lyalin, N. Martensson, A. B. Preobrajenski, *ACS Nano* **2015**, *9*, 8997; b) K. A. Simonov, N. A. Vinogradov, A. S. Generalov, E. M. Zagrebina, N. Martensson, A. A. Cafolla, T. Carpy, J. P. Cunniffe, A. B. Preobrajenski, *J. Phys. Chem. C* **2014**, *118*, 12532.

[15] I. Horcas, R. Fernández, Gómez-Rodríguez, J. Colchero, J. Gómez-Herrero, A. M. Baro, *Rev. Sci. Instrum.* **2007**, *78*, 013705.

[16] J. Perdew, K. Burke, M. Ernzerhof, *Phys. Rev. Lett.* **1996**, *77*, 3865.

[17] S. Grimme, J. Antony, S. Ehrlich, H. Krieg, *J. Chem. Phys.* **2010**, *132*, 154104.

[18] G. Lippert, J. Hutter, M. Parrinello, *Mol. Phys.* **1997**, *92*, 477.

[19] J. VandeVondele, M. Krack, F. Mohamed, M. Parrinello, T. Chassaing, J. Hutter, *J. Comput. Phys. Commun.* **2005**, *167*, 103.

Received: November 2, 2016
Revised: December 16, 2016
Published online: January 25, 2017

